Nature Environment and Pollution Technology
An International Quarterly Scientific Journal

p-ISSN: 0972-6268
(Print copies up to 2016)
e-ISSN: 2395-3454

Vol. 23 | No. 3 | pp. 1839-1848 | 2024

Original Research Paper

https://doi.org/10.46488/NEPT.2024.v23i03.056

Open Access Journal

Effect of Rice Biochar on Typical Cadmium, Lead and Zinc Form in Contaminated Soil in Northwest Guizhou Province, China

Ji Wang*, Die Xu, Xiongfei Cai*† and Shuai Zhao*****

*School of Geographic and Environmental Sciences, Guizhou Normal University, Guiyang, 550025, China
**School of Education Science, Qiannan Normal University for Nationalities, Duyun, 558000, China
***School of Environmental Science and Engineering, Dalian Maritime University, Dalian, 116000, China
†Corresponding author: Xiongfei Cai; ddwll5201@163.com

Nat. Env. & Poll. Tech.
Website: www.neptjournal.com

Received: 14-11-2023
Revised: 13-12-2023
Accepted: 11-01-2024

Key Words:
Rice biochar
Historical pollution soil
Heavy metals
Passivation repair

ABSTRACT

This study was conducted in Hezhang County, Bijie City, Guizhou Province. The soil in the zinc smelting area has been contaminated with cadmium, lead, and zinc. Therefore, these elements are the focus of this research. Rice husk biochar was used as the passivation material. The Fourier infrared spectrum was utilized to study the biochar's morphology, element content, mineral composition, structure, and surface functional groups. Moreover, the physical and chemical properties of the biochar were analyzed to explore its passivation effect. Biochar is beneficial in the cleaning of cadmium, lead, and zinc minerals and can be used for the passivation of heavy metals in contaminated soil. This study aims to understand the detailed mechanism behind this process and provide experimental data and ideas for pollution control. The results indicate that the biochar contains many functional groups, including -OH, C-H, C-O, C=O, C=C, and C-O-C. It also consists of a significant quantity of potassium salt, calcite, and quartz. Biochar has a noticeable pore structure, and as the pyrolysis temperature increases, the pore structure becomes more developed and thinner, with a smooth surface. The main minerals in the soil are quartz, mica, zeolite, illite, and chlorite. The aromatic degree of biochar increased with pyrolysis temperature. In contrast, the aromatic degree and polarity first increased and then decreased. The 0.2-0.45 mm biochar exhibited the best passivation effect on cadmium, lead, and zinc.

INTRODUCTION

Soil is an important part of the human living environment. However, due to the rapid expansion of modern society, many heavy metal pollutants released during mining have contaminated the soil, resulting in severe soil heavy metal pollution. According to the 2014 National Soil Pollution Survey Bulletin, the soil is predominantly polluted by inorganic pollutants. Of all the sites with pollutant levels exceeding the limit, 82.8% are affected by inorganic pollutants. Among these, cadmium (Cd) is the primary heavy metal contaminant in China's soil, with an over-limit rate of 7%. The over-limit rates of lead (Pb) and zinc (Zn) are 1.5% and 0.9%, respectively (MEP & MLR 2014).

The zinc smelting industry in northwestern Guizhou Province has a history of more than 300 years. Historically, there was a greater focus on development than on environmental protection. This outdated smelting technique contributed to economic growth but at a significant environmental cost. Inadequate waste treatment led to the release of large quantities of toxic exhaust gases, soot, and heavy metal pollutants such as Cd, Pb, and Zn. These pollutants were discharged during smelting, causing serious soil contamination. As a result, over 20 million tons of waste and 1200 hectares of soil remain untreated (Lin 2009). To remediate and treat these contaminated areas, it is urgent to find appropriate methods.

At present, studies on heavy metal-contaminated soils in the historical legacy of zinc refining in northwest Qianxi primarily focus on investigating the current state of soils in the contaminated area. These studies analyze the distribution of heavy metal morphology and geochemical transport characteristics and evaluate the biological effectiveness of heavy metals in soils within the historically contaminated area using relevant methods and predictive models. They also explore the soil-crop system in the legacy contaminated area by heavy metals. However, there are few studies on the use of chemical passivation agents to remediate soil in the historical legacy of zinc refining in northwest Qianxi (Yang et al. 2003, Lin et al. 2009, Ao et al. 2009, Gao et al. 2017, Zhang et al. 2017a, Sun et al. 2013, Liu et al. 2020, Sun et al. 2006, Kang et al. 2015)

Soil remediation methods for heavy metal contamination can be divided into physical remediation, chemical remediation, and bioremediation (Derakhshan et al. 2017). Among chemical methods, in situ passivation remediation has received wide attention due to its high operability, cost-effectiveness, and suitability for large-scale applications. In recent years, it has become a research hotspot for remediating soil polluted by heavy metals (Li et al. 2019).

Passivators used for treating soil with heavy metals are often categorized into inorganic passivators (such as lime, phosphate, metals and their oxides, and clay minerals) and organic passivators (including organic waste, organic acids, and biochar) (Zhao et al. 2021). Biochar, a highly carbon-containing aromatized solid material prepared by pyrolysis under anoxic and relatively low-temperature conditions, is particularly effective. It has a complex pore structure, a large specific surface area, and abundant surface functional groups, making it excellent at absorbing and immobilizing heavy metal pollutants. Consequently, biochar has become a research hotspot in the environmental field in recent years (Shi et al. 2019).

According to the Ministry of Agriculture and Rural Affairs of China, current agricultural straw resources in China mainly include rice, corn, and wheat, which together account for 83.51% of the total straw resources. In 2021, China produced 900 million tons of straw, ranking first in the world.

Moreover, the production is increasing at an annual rate of 3%, providing sufficient raw material for biochar. Therefore, biochar is a green and reasonable solution for recycling agricultural straw resources (Wei et al. 2019, Xie et al. 2010, Meng et al. 2018). Currently, many studies have analyzed biochar's passivation effects on the remediation of soil polluted by heavy metals. However, most of them regard biochar as a homogeneous body and do not consider the influence of different sizes of biochar particles. Therefore, it is necessary to investigate biochar's passivation effects on the remediation of polluted soil with different particle sizes. In the soil of the historical legacy of zinc refining in northwestern Qianxi, this investigation has practical application significance and aligns with the current development trend of national environmental ecology.

This paper focuses on the historical Zn refining area in northwest Guizhou province, where heavy metals, including Cd, Pb, and Zn, have contaminated the soil. The rice husk biochar was used as the test material for passivation remediation. We analyzed the biochar and the test soil samples using characterization techniques such as scanning electron microscopy, Fourier infrared spectroscopy, X-ray diffraction, specific surface area measurement, and organic elemental analysis. The study investigated the differences in the morphological structure, elemental content composition, and surface functional groups of the biochar. This paper aims to provide basic experimental data and pollution prevention ideas by investigating the rice husk biochar's passivation effects on soil contaminated by heavy metals.

MATERIALS AND METHODS

Test Materials

The test soil was obtained from a 0-20 cm soil layer of a vegetable field in a soil refining area of Hezhang County, Bijie City, Guizhou Province. The collected soil samples were mixed well in a sealed bag, brought back to the laboratory, and laid flat on kraft paper. A rubber hammer was used to break up the lumpy soil to prevent clumping. After removing impurities, the samples were dried naturally at room temperature. The dried samples were then filtered through a 2 mm nylon sieve and sealed in bags for use. The basic physical and chemical properties are as follows: the soil type was loam, the moisture content after air-drying was 4.75%, the pH was 7.51, indicating weak alkalinity and the conductivity was 155.11 $\mu s.cm^{-1}$, cation exchange was 8.78 $cmol(+).kg^{-1}$, soil organic matter content was 36.89 $g.kg^{-1}$, total N and total P are 0.05 and 1.00 $g.kg^{-1}$, respectively. The total amounts of Cd, Pb, and Zn were 14.07, 4518.15, and 71,786.83 $mg.kg^{-1}$, respectively. The rice husk biochar products, which were prepared by pyrolysis at 300°C, 400°C, and 500°C, are noted as W300, W400, and W500, respectively. They were purchased from Henan Lize Environmental Protection Technology Co, with sizes of 0.075-0.2mm, 2: 0.2-0.45mm, and 3: 0.45^{-1}mm. Their basic physicochemical properties are shown in Table 1.

The aromaticity, hydrophilicity, and polarity magnitudes of biochar can be expressed by the ratios of the organic

Table 1: Physical and chemical properties of biochar.

Biochar type	Water content	pH	EC [μs. cm^{-1}]	Ash	Specific surface area[$m^2.g^{-1}$]	Total pore volume [$cm^3.g^{-1}$]	Average pore size[nm]	C[%]	H[%]	N[%]	O[%]	S[%]
W300	3.67%	11.56	8475	53.51%	61.89	0.166	4.39	28.24	2.77	0.43	8.36	0.58
W400	3.88%	10.44	5335	51.88%	67.53	0.165	4.25	34.80	1.07	0.54	9.62	0.73
W500	0.67%	12.28	14500	50.21%	130.28	0.309	4.90	42.59	1.34	0.75	12.37	1.05

components' H/C, O/C, and (O+N)/C. The ratio of H/C atoms is negatively correlated with the degree of biochar aromaticity (Lin et al. 2017). Conversely, the ratios of O/C and (O+N)/C are positively correlated with the aromaticity and polarity of biochar (Chen et al. 2013, Wu et al. 2015, Hseu 2006). Based on the analysis of organic elements in rice husk biochar, the aromaticity of rice husk biochar in this study increased with temperature. The aromaticity and polarity showed an increasing trend before experiencing a downturn.

Material Characterization Analysis

Soil mineral types were analyzed using an X-ray diffractometer (XRD) (BrukerD8advance, Bruker, Germany). The surface morphology of biochar was determined using a scanning electron microscope (SEM) (ZEISSGemini300, Carl Zeiss AG, Germany). The organic elemental composition of biochar was analyzed with an organic elemental analyzer (EA) (ElementarvarioEl III, Erimenta, Germany). A fully automatic specific surface and porosity analyzer (BET) (McASAP2460, McMurritic Instruments Co., Ltd., USA) was used to determine the specific surface area, pore size, and pore volume of the biochar. A Fourier infrared spectrometer (FTIR) (FTIR-850 Ltd.) was used to qualitatively analyze the surface functional groups of biochar.

Design of Experiments

The experiment was conducted on January 14, 2021, at the Key Laboratory of Karst Mountain Ecology and Environment of Guizhou Normal University. It aimed to analyze the soil's static passivation. The soil in the pots was mixed with biochar. First, an appropriate amount of ultra-pure water was added to the pots to moisten the soil to 60% of the field water-holding capacity. During incubation, lost water was replenished using the weighing method. After 100 days of incubation, the soil samples were removed, air-dried, ground, and sieved for analysis and testing.

Analytical Methods and Instruments

Using the potentiometric method (water-soil ratio 2.5:1), the soil's pH was determined by the pH meter (PHS-320, Shanghai Yidian Scientific Instruments Co., Ltd.). Soil electrical conductivity refers to the electrical conductivity of a solution within a unit distance. Using the electrode method, the soil's electrical conductivity (EC) was determined by the electrical conductivity meter (DDSJ-308F, Shanghai Yidian Scientific Instruments Co., Ltd.). Cation exchange capacity (CEC) is a measure of the total negative charges within the soil that adsorb plant nutrient cations. The leaching-spectrophotometric method, adopting hexamine-cobalt trichloride, was used to determine the soil's cation exchange capacity (CEC). The automatic interrupted chemical analyzer (CleverChem200+, DeChem-Tech GmbH, Germany) was used to determine the total nitrogen (TN) and total phosphorus (TP), using sulfuric acid boiling sodium salicylate and sulfuric acid boiling-molybdenum antimony resistance, respectively. The ultraviolet-visible spectrophotometer (UV-5500, Shanghai Yuananalysis Instruments Co., Ltd.) was used to determine the content of soil organic matter (SOM) using the hydrated thermal potassium dichromate oxidation-colorimetric method. The total amount of soil Cd, Pb, and Zn was evaluated using tetraacid digestion (HCl-HNO3-HF-HClO4), the plant active Cd, Pb, and Zn (DTPA-Cd, DTPA-Pb, and DTPA-Zn) were extracted using diethylenetriaminepentaacetic acid (DTPA) leaching. The toxic leached Cd, Pb, and Zn (TCLP-Cd, TCLP-Pb, and TCLP-Zn) were extracted by acetic acid (CH3COOH). The total amount and the other two forms were determined by the flame atomic absorption spectrometer (GGX-800, Beijing Haiguang Instruments Co., Ltd.).

Data Processing

Excel 2019 was used for data processing and calculation, and Origin 2019 b was used for the plotting.

RESULTS AND DISCUSSION

Effect of Biochar on Soil Physicochemical Properties

Biochar W3 (300), W2 (400), W2 (500), and W3 (500) treatments have clear effects of pH reduction. However, biochar of different particle sizes generates different results of soil CEC. The CEC in soil treated by rice husk biochar at 300°C increased first and then decreased as the biochar's particle size grew. While at 400°C, the CEC showed a descending trend along with the increase of the biochar's particle size. At 500°C, the CEC trend was opposite to that at 400°C. The W3 (500) treatment resulted in the highest CEC of 9.16 $cmol^{+}.kg^{-1}$, followed by the W2 (300) treatment. At 400°C, the maximum CEC of the rice husk biochar treatment was 8.92 $cmol^{+}.kg^{-1}$. At 300°C and 400°C, the EC of soil treated with rice husk biochar tended to decrease as the biochar particle size decreased. At 300°C and 400°C, the CEC of soil treated with rice husk biochar decreased as biochar particle size reduced. However, the EC of soil in the W2(500) treatment was the largest and could reach 466.21 $\mu s.cm^{-1}$ (Table 2).

Effect of Biochar on the Effective State Cd, Pb, and Zn Content

The total content of heavy metals in soil indicates their potential hazard. The DTPA-extracted state of heavy metals is closely related to the plant-available fraction. It can be used

Table 2: Physical and chemical properties of soil under different treatments.

Processing Category	pH	CEC [$cmol^{+}.kg^{-1}$]	EC [$\mu s.cm^{-1}$]	TN [$mg.kg^{-1}$]	TP [$g.kg^{-1}$]
CK	7.51	8.78	155.11	46.67	1.00
WF(300)	7.38	8.39	355.71	2.00	0.61
W1(300)	7.41	8.15	318.71	87.23	0.23
W2(300)	7.46	8.93	302.21	19.19	0.23
W3(300)	7.19	7.19	262.71	8.91	0.72
WF(400)	7.38	8.92	334.21	52.54	0.59
W1(400)	7.35	8.52	375.71	18.07	0.38
W2(400)	7.25	8.07	266.21	10.16	0.53
W3(400)	7.30	6.96	167.81	5.72	0.48
WF(500)	7.44	7.65	446.71	15.41	0.24
W1(500)	7.46	7.74	367.71	26.55	0.22
W2(500)	7.17	6.68	466.21	26.97	0.26
W3(500)	7.22	9.16	346.71	-	0.71

Note: "-" means not detected.

to measure the content of heavy metal elements in soil that are effective for plants (Cao et al. 2009). Effective state Cd, Pb, and Zn in soil accounted for 28.57%, 24.47%, and 7.51% of the total, respectively. Biochar has the most significant effect on the content of DTPA-Pb in soil (Fig. 1). Under the W1 (400) treatment, the content of DTPA-Cd is reduced by 15.85%. Under the W2 (300) treatment, the reduced percentages of DTPA-Pb and DTPA-Zn were 40.92% and 23.94%, respectively. Overall, biochar with a size of 0.2-0.45 mm had the most significant effect on all three heavy metals in their effective states. Pb is less mobile in soil and has a strong affinity for the soil's mucilage and organic matter. Even under acidic conditions, Pb is easily precipitated with phosphoryl chloride (Sauve et al. 2000). Previous studies have shown that different factors can account for the solid phase-solution partitioning of heavy metals in soil (Buchter et al. 1989, Gao et al. 2018).

Effect of Biochar Addition on the Content of TCLP-Cd, Pb, and Zn

The TCLP method (Toxicity Characteristic Leaching Procedure) can easily, quickly, and effectively evaluate the ecological risk of heavy metals in solids and is often used to assess soil heavy metal pollution and remediation effects (Wu et al. 2017). TCLP-Cd, Pb, and Zn accounted for 17.27%, 35.77%, and 24.8% of the total, respectively (Fig. 2). The passivation effect of different particle size biochar treatments on toxic leaching state heavy metals was similar to that of the effective state. The passivation effect on Pb and Zn was better than that on Cd. The W2(400) treatment showed the

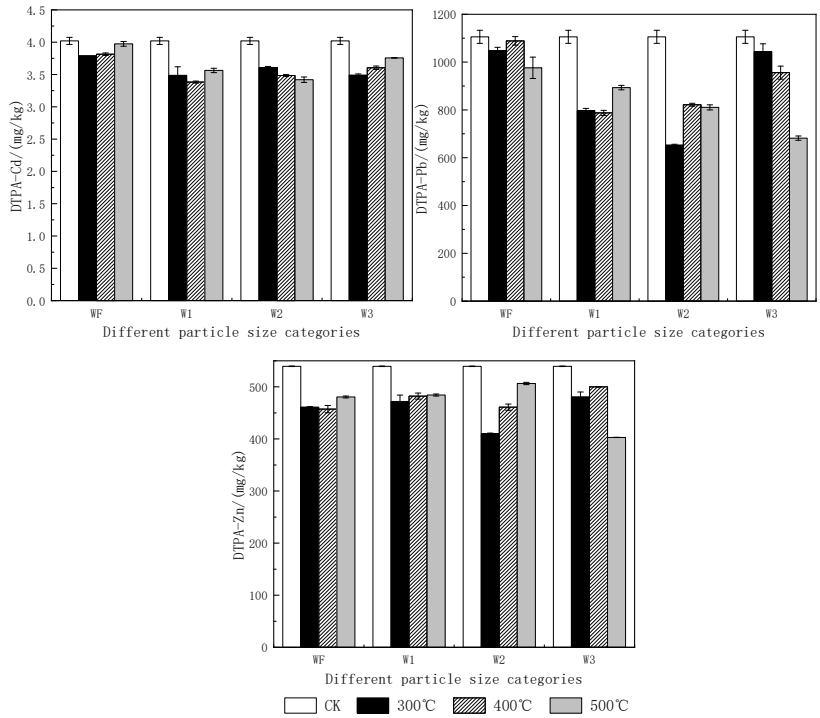

Fig. 1: Changes of DTPA-Cd, Pb, and Zn contents after different rice biochar treatments.

best passivation effect on Cd and Zn, reducing TCLP-Cd and TCLP-Zn by 25.81% and 36.13%, respectively. The W2(300) treatment demonstrated the best passivation effect on TCLP-Pb, with a reduction rate of 51.62%. Overall, biochar with a size of 0.2-0.45 mm had the most significant passivation effect, significantly reducing the two effective forms of the three heavy metals.

Characterization and Analysis of Biochar and Soil Samples

X-ray diffraction analysis: According to the X-ray diffraction analysis, the minerals contained in the test soil mainly included quartz, feldspar, mica, zeolite, illite, and chlorite (Fig. 3). The surface of some minerals in the soil could adsorb and immobilize heavy metals, thereby reducing their mobility and impact on the environment (Miguel et al. 2002, Li et al. 2007). In this study, the rice husk biochar primarily contained potassium salt (KCl), calcite ($CaCO_3$), and quartz (SiO_2). This finding is consistent with the research of Liu et al. (2017) and Zhong et al. (2019). The sharp diffraction peaks in the plots mainly represented inorganic crystals SiO_2 (Zhong et al. 2019), $CaCO_3$, and KCl. SiO_2 corresponded to the highest diffraction peak, indicating that its content was greater than that of the other inorganic compounds. As the pyrolysis temperature increased, inorganic ions such as SiO_2, Ca, K, and Mg sintered and fused into inorganic minerals and alkali metals. At higher temperatures, the presence of K converts some Ca elements into silicates, which may lead to a decrease in $CaCO_3$ (Zhang et al. 2017b). The characteristic peaks of cellulose and hemicellulose appeared at 2θ = 15-20° (Feng et al. 2009). During the charring of biochar, these characteristic peaks gradually widened, and their intensity decreased as the temperature increased. The charring process destroyed the microcrystalline structure of cellulose, and the volatile components continued to escape. At lower temperatures, the biochar made from rice straw lacked characteristic peaks of cellulose and was amorphous. The characteristic peaks at 26° and around 43° correspond to the (002) and (100) crystalline surfaces of graphite, reflecting the degree of graphitization.

After charring, as the temperature increased, the diffraction peaks of the rice husk biochar shifted toward

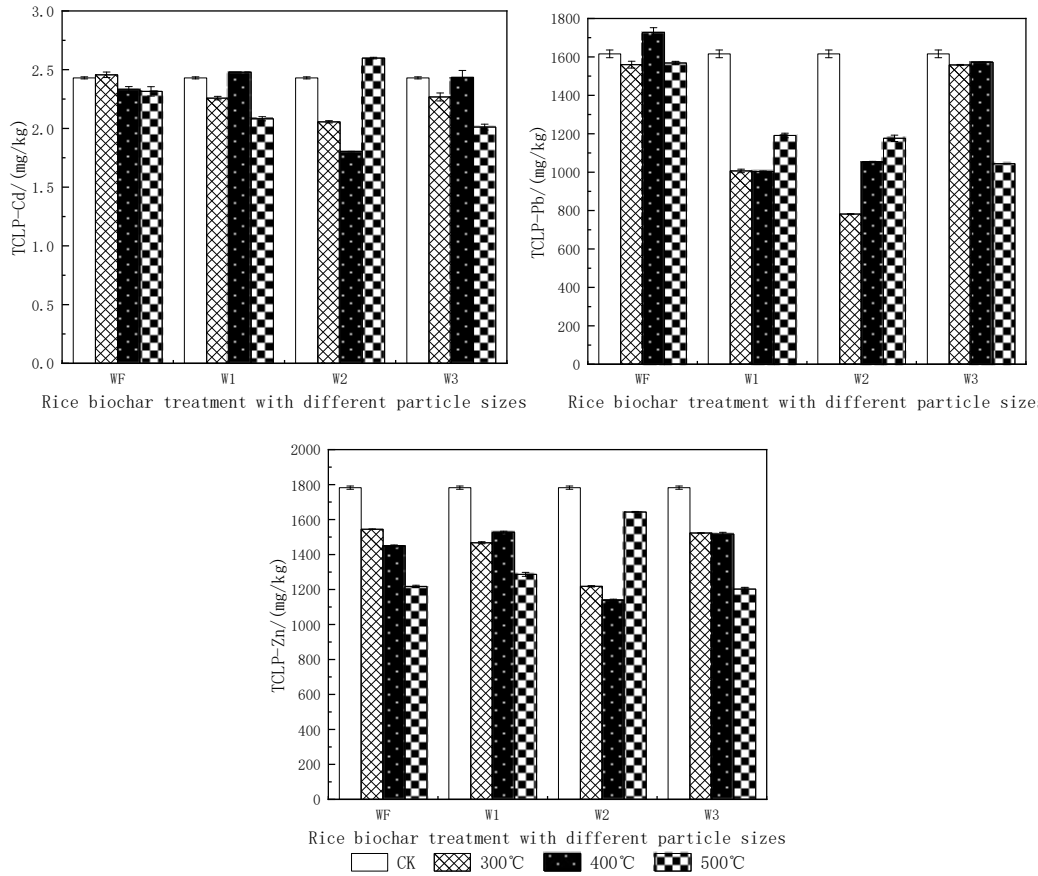

Fig. 2: Changes of TCLP-Cd, Pb, and Zn contents after different rice biochar treatments.

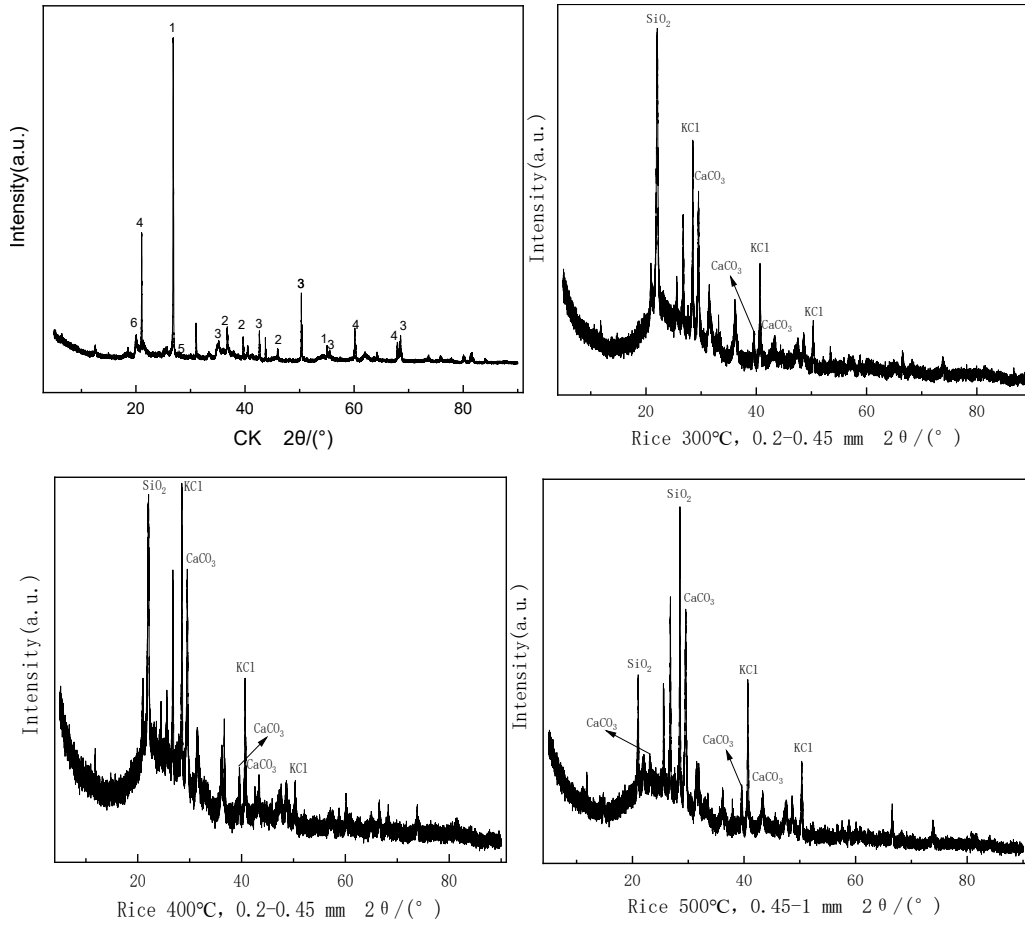

1: Quartz (SiO_2), 2: Feldspar (SiO_2, Al_2O_3, K_2O, Fe_2O_3, Na_2O, CaO), 3: Mica ($KAl_2(AlSi_3O_{10})(OH)_2$), 4: Zeolite ($Na(AlSi_2O_6)\cdot H_2O$, $Ca(Al_2Si_3O_{10})\cdot 3H_2O$), 5: Illite ($KAl_2[(SiAl)_4O_{10}]\cdot(OH)_2\cdot NH_2O$), 6: Chlorite ($Y_3[Z_4O_{10}](OH)_2\cdot Y_3(OH)_6$) (Y: mainly represents Mg, Fe & Al; Z: mainly Si and Al)

Fig. 3: XRD patterns of CK and three kinds of biochar.

higher theta angles. Due to further charring of the biomass, the aromaticity of carbon increased, and the stacking mode between aromatic lamellae tended to become more ordered. Therefore, biochar prepared at high temperatures had less volatile organic carbon and more aromatized carbon. The functional groups remaining on the carbon structure were more stable, enhancing the chemical stability of the biochar. This explains why biochar is suitable for the passivation of heavy metals in contaminated soil and benefits remediation (Lin et al. 2016, Ma 2019). Rice prefers Si and absorbs a large amount of Si during its life cycle. Therefore, rice husk is rich in Si, consistent with previous research (Liang et al. 2006, Wu & Gong 2010, Xiao et al. 2014). The broad half-peak of the diffraction indicated that the prepared biochar particles were small and rich in irregular pores, which helped increase the specific surface area of the material (Yu et al. 2019).

Swept surface electron microscopy analysis: The scanning electron microscope showed the images of rice husk biochar (Fig. 4). At different pyrolysis temperatures, all the images of biochar exhibited obvious pore structures. However, the degree of porosity varied. When the pyrolysis temperature was 300°C, the rice husk biochar was flaky without well-developed pores. Instead, the pores were few and irregular, and the surface of the biochar was covered with granular material. When the temperature was raised to 400 or 500°C, the rice husk biochar had a more developed pore structure. The structure was evenly distributed with stable sized round pores with a smooth and flat surface. The biochar became lighter and thinner, which was good for the passivation and fixation of heavy metal pollutants.

Fourier infrared spectral analysis: The preparation of biochar by pyrolysis had four steps: water evaporation, transition, decomposition of organic matter, and charring. In this study, the rice biochar consisted of hemicellulose, cellulose, and lignin. The cracking temperature of different components varied. Hemicellulose could be cracked at low

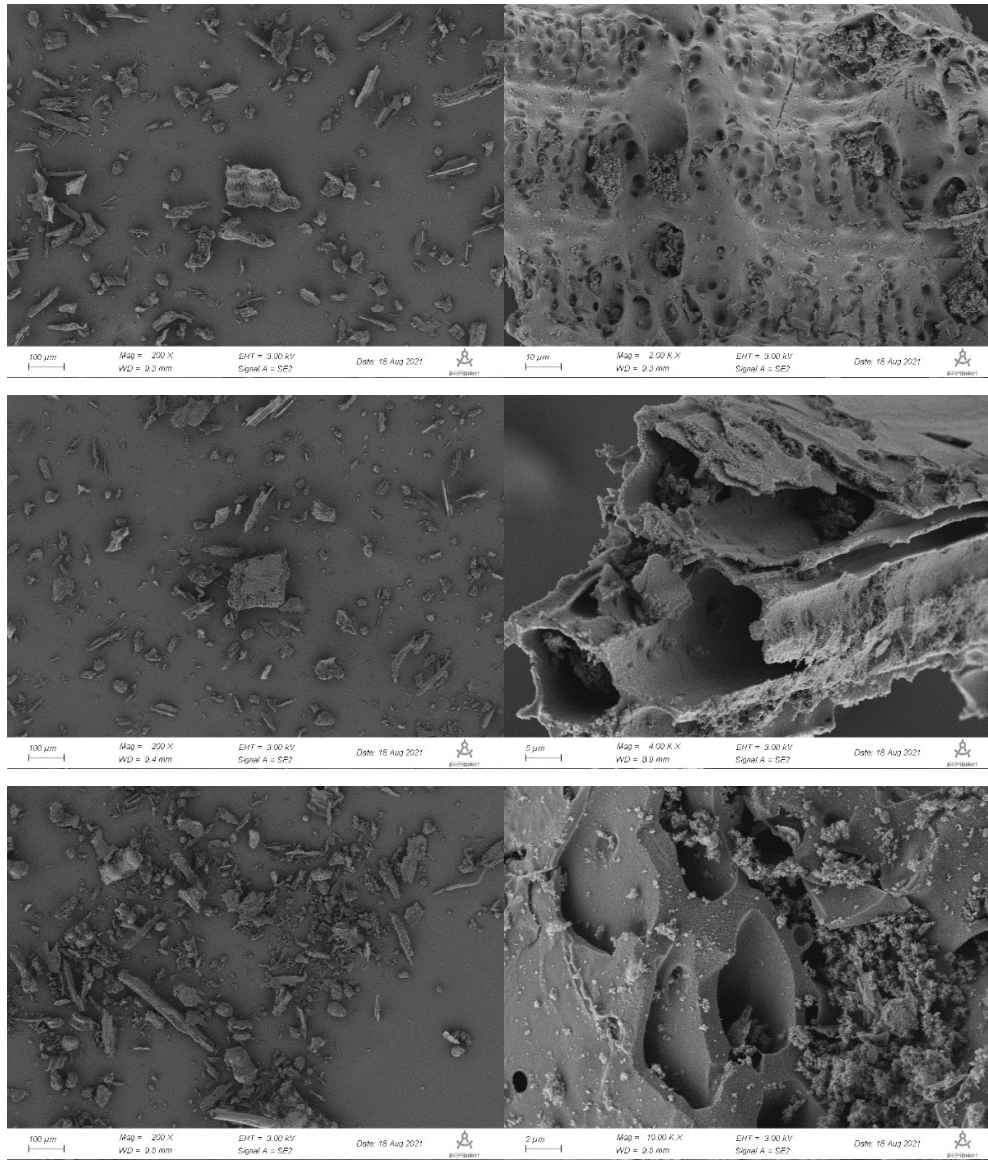

Fig. 4: SEM image of W2(300), W2(400) and W3(500).

temperatures, and cellulose and lignin gradually started to decompose as the pyrolysis temperature increased (Jian et al. 2015). From the analysis of IR spectra (Fig. 5), the surface of rice husk biochar contained functional groups such as carbonyl, hydroxyl, methylene, and aromatic rings (Zhu et al. 2021). At 3440 cm^{-1}, there was a broad and strong absorption peak. The absorption peak in this band can be explained by the hydrogen-bonded phenolic hydroxyl-OH stretching vibration. The effect of pyrolysis' temperature effect on this absorption peak was not significantly obvious. At 2939 cm^{-1}, there was an absorption peak with lower intensity. This was caused by the asymmetric C-H stretching vibration of the aliphatic methylene CH2. The source of this functional group included aliphatic compounds, alicyclic compounds, and carbohydrates in organic matter. The weakening of the peak intensity of rice husk biochar at 400 and 500°C might be related to the decomposition of aliphatic-CH2 (Chun et al. 2004). The functional groups at 1644 cm^{-1} were polycyclic aromatic hydrocarbons C =C and C=O (Que et al. 2018). The absorption peak functional group at 1428 cm^{-1} was methylene-CH2. The absorption peak functional group at 1104 cm^{-1} was caused by cellulose or hemicellulose C-O-C (Keiluweit et al. 2010). In this study, the functional groups C=C, C=O, and C-H were higher in rice husk biochar at

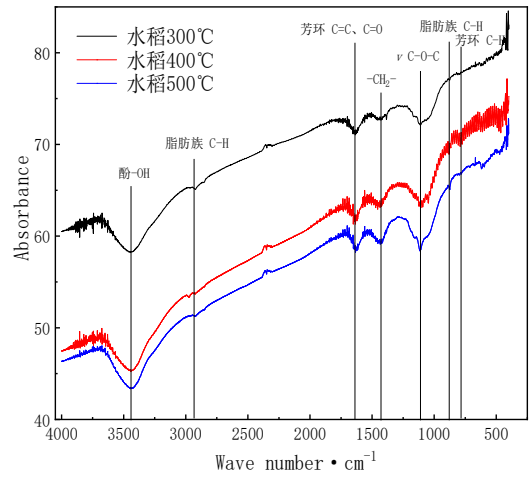

Fig. 5: FTIR spectra of the biochars.

300 °C and 400 °C. However, the original composition and structure in rice husk biochar were gradually decomposed at 500 °C. High temperatures significantly reduced the number of functional groups. The oxygen-containing functional groups -OH and C=O could react with heavy metal ions (Chen et al. 2008, Torri & Fabbri 2014). The absorption peaks at 888 and 788 cm^{-1} were caused by the bending vibrations of the aromatic ring C-H. The absorption peaks of rice husk biochar increased with pyrolysis temperature, indicating that the aromatic rings were formed and the aromatization increased during the pyrolysis. This was consistent with the results of organic elemental analysis.

CONCLUSION

1. Biochar had little effect on soil pH. Biochar with different particle sizes had variable effects on the soil's CEC. Under W3(400) treatment, the CEC of soil became as high as 9.16 $cmol.kg^{-1}$. W2(500) treatment achieved the best effect on the soil's EC, which increased by 466.21 $\mu s.cm^{-1}$.
2. Rice husk biochar had a better passivation effect on DTPA-Pb compared to others. Under the W2(300) treatment, the content of DTPA-Pb was reduced by 40.92%. When heavy metals were in a toxic leaching state, the biochar's passivation effects were better for Pb and Zn than for Cd. The W2(400) treatment reduced the TCLP-Cd and TCLP-Zn contents by 25.81% and 36.13%, respectively. The W2(300) treatment was the most effective for TCLP-Pb, reducing it by 51.62%. The medium-sized rice husk biochar, which was 0.2-0.45 mm, had the best passivation effect on all three heavy metals.
3. According to the characterization analysis, the minerals in the test soil included quartz, feldspar, mica, zeolite, illite, and chlorite. The rice husk biochar contained KCl, $CaCO_3$, and SiO_2, with SiO_2 being more prevalent than the other inorganic compounds. Scanning electron microscope images showed that rice husk biochar at 300°C was flaky, with an underdeveloped pore structure. As the pyrolysis temperature increased, the biochar became lighter and thinner, with more developed pores and smoother surfaces. The functional groups in the rice husk biochar included carbonyl, hydroxyl, methylene, and aromatic rings.

Future research should focus more on natural environment experiments to investigate the in situ remediation effects of biochar on polluted sites. The duration of passivation should be adjusted to measure the content of different forms of heavy metals at various time points. The dynamic changes in heavy metals over different time ranges should be explored. It is also recommended to study the relationship between biochar aging and its passivation effect.

ACKNOWLEDGEMENTS

This work was supported by the Technology Foundation, Guizhou Province (Qian Sci. Co., [2019], NO.1231).

REFERENCES

Ao, Z. Q., Lin, W. J., Yan, C. L., Qu, L. Y., Xiao, T. F. and Lin, K. 2009. Speciation and transformation of heavy metals in the indigenous zinc smelting area. J. Ecol. Environ. Sci., 18(3): 899-903.

Buchter, B., Davidoff, B. and Amacher, M. C. 1989. Correlation of Freundlich Kd and n retention parameters with soils and elements. J. Soil Sci., 148(5): 370-379.

Cao, X. D., Wahbi, A. and Ma, L. 2009. Immobilization of Zn, Cu, and

Pb in contaminated soils using phosphate rock and phosphoric acid. J. Hazard. Mater., 164(2): 555-564.

Chen, B. L., Zhou, D. D., Zhu, L. Z. and Shen, X. Y. 2008. The adsorption effect of biochar adsorbent on organic pollutants in water mechanism. Sci. Sin. Chim., (6): 530-537.

Chen, Z. M., Chen, B. L. and Zhou, D. D. 2013. Composition and sorption properties of rice-straw derived biochars. Acta Sci. Circumst., 33(1): 9-19.

Chun, Y., Sheng, G. Y. and Chiou, C. T. 2004. Compositions and sorptive properties of crop residue-derived chars. Environ. Sci. Technol., 38(17): 4649-4655.

Derakhshan, N. Z., Jung, M. C. and Kim, K. H. 2017. Remediation of soils contaminated with heavy metals with an emphasis on immobilization technology. Environ. Geochem. Health, 40: 927-953.

Feng, X. and Ju, C. H. H. 2009. Comparison of biosorbents with inorganic sorbents for removing copper(Ⅱ) from aqueous solutions. J. Environ. Manage., 90(10): 3105-3109.

Gao, H., Song, J., Lv, M. C., Zhang, X., Zhang, Q., Liu, L. F. and Log, J. 2017. Evaluation of cadmium phytoavailability in soils from a zinc smelting area in Hezhang County, Guizhou Province, using diffusive gradients in thin films and conventional chemical extractions. J. Agro-Environ. Sci., 36(10): 1992-1999.

Gao, P., Chen, Y. and Liang, Y. 2018. Study of the aging effect on the stability of biochar initially adsorbed Cd(II). Acta Sci. Circumst., 38(5): 1877-1884.

Hseu, Z. Y. 2006. Extractability and bioavailability of zinc over time in three tropical soils incubated with biosolids. Chemosphere, 63: 762-771.

Jian, M. F., Gao, K. F., Yu, H. P. and Yang, Y. 2015. Comparison of surface characteristics and cadmium solution adsorption capacity of un-acidified or acidified bio-chars prepared from rice straw under different temperatures. J. Ecol. Environ. Sci., 24(8): 1375-1380.

Keiluweit, M., Nico, P. S. and Johnson, M. G. 2010. Dynamic molecular structure of plant biomass-derived black carbon (biochar). Environ. Sci. Technol., 44(4): 1247-1253.

Kang, H. J., Lin, J., Zhang, N. M., Bao, L. and Liu, B. S. 2015. Passivation effect of different passive materials on heavy metal polluted soil. Chin. Agric. Sci. Bull., 31(35): 176-180.

Li, K. W., Wu, Y. X., Huang, Z. M., Fan, R. and Li, J. F. 2007. Measurement results comparison between laser particle analyzer and sieving method in particle size distribution. China Powder Sci. Technol., (5): 10-13.

Li, Y., Zhu, S. H., Shang, J. Y. and Huang, Y. Z. 2019. Immobilization materials for cadmium and arsenic-contaminated soil remediation and their scientific metrology.

Liang, Y. C., Hua, H. X. and Zhu, Y. G. 2006. Importance of plant species and external silicon concentration to active silicon uptake and transport. New Phytol., 172(1): 63-72.

Lin, J. Y., Zhang, Y., Liu, Y., Xia, J. J. and Tong, Sh.T. 2016. Structure and properties of biochar under different materials and carbonization temperatures. Chin. J. Environ. Eng., 10(6): 3200-3206.

Lin, Q. Y., Jiang, C. C. and Zhang, M. Y. 2017. Characterization of the physical and chemical structures of biochar under simulated aging conditions. Environ. Chem., 36(10): 2107-2114.

Lin, W. J. 2009. Ecological degeneration and heavy metals pollution in zinc smelting areas. Ecol. Environ. Sci., 18(1): 149-153.

Lin, W. J., Xiao, T. F., Zhou, W. C., Ao, Z. Q. and Zhang, J. F. 2009. Environmental concerns on geochemical mobility of lead, zinc, and cadmium from zinc smelting areas: Western Guizhou, China. Environ. Sci., 30(7): 2065-2070.

Liu, Y. X., Yang, S. and Wang, Y. Y. 2017. Bio-and hydrochars from rice straw and pig manure: Inter-comparison. Bioresour. Technol., 235: 332-337.

Liu, H., Wu, Y. G., Luo, Y. F. and Wu, P. 2020. Effects of different organic acid-phosphate rock powder composites on the immobilization of heavy metals in waste slags of indigenous smelting zinc. Earth Environ., 48(2): 258-267.

Ma, S. 2019. Physicochemical properties of rice straw biochar under the same temperature treatment and its impact on soil heavy metals the impact of genus bioavailability. Yangzhou: Yangzhou University.

Meng, Q. J., Liu, Y., Li, P. F., Liang, S. C. and Zhang, Y. 2018. Study on adsorption characteristics and mechanism of biochar on trichloroethylene. J. Environ. Sci., 49(12): 36-43.

Miguel, A. M., Marti and Montero, S. 2002. Laser diffraction and multifractal analysis for the characterization of dry soil volume-size distributions. Soil Tillage Res., 64(1-2): 113-123.

MEP and MLR 2014. Announcement on national soil pollution survey. Available at https://english.www.gov.cn/policies/latest_releases/2014/08/23/content_281474983026954.htm

Que, W., Zhou, Y. H. and Liu, Y. G. 2018. Appraising the effect of in-situ remediation of heavy metal contaminated sediment by biochar and activated carbon on Cu immobilization and microbial community. Ecol. Eng., 127: 519-526.

Sauve, S., Hendershot, W. and Allen, H. E. 2000. Solid-solution partitioning of metals in contaminated soils: Dependence on pH, total metal burden, and organic matter. Environ. Sci. Technol., 34(7): 1125-1131.

Shi, Z. L., Wang, F., Wang, J. C., Li, X., Sun, R. H. and Song, C. J. 2019. Utilization characteristics, technical model, and development suggestion on crop straw in China. J. Agric. Sci. Technol., 21(5): 8-16.

Sun, L., Yang, Y. G., Bai, W. Y., Bi, X. Y. and Jin, Z. S. 2006. Heavy metal accumulation in natural plants in the zinc smelting area in northwestern Guizhou Province. Earth Environ., (2): 61-66.

Sun, L., Zhao, L., Zhang, L. J., Shi, C. M., Zhu, X. W. and Wang, K. Y. 2013. Cadmium pollution caused by artisanal zinc-smelting in Hezhang County. Chin. J. Public Health., 29(4): 541-543.

Torri, C. and Fabbri, D. 2014. Biochar enables anaerobic digestion of aqueous phase from intermediate pyrolysis of biomass. Bioresour. Technol., 172: 335-341.

Wei, H. J., Yang, Q., Li, J. S., Yang, H. P. and Chen, H. P. 2019. Analysis of spatiotemporal and density changes of crop straws resources in China. Renew. Energy Resour., 37(9): 1265-1273.

Wu, J. R. and Gong, J. Y. 2010. Research progress on silicon nutrition in rice. China Rice, 16(3): 5-8.

Wu, S. X., Wang, X., Chen, C., Peng, B., Tan, C. Y., Zhang, F., Xu, Y. Q. and Zhang, Y. J. 2015. Characterization of biochar derived from water hyacinth, rice straw, and sewage sludge and their environmental implications. Environ. Chem., 35(12): 4021-4032.

Wu, T., Li, X. P., Cai, Y., Ai, Y. W., Sun, X. M. and Yu, H. T. 2017. Geochemical behavior and risk of heavy metals in different size lead-polluted soil particles. China Environ. Sci., 37(11): 4212-4221.

Xiao, X., Chen, B. L. and Zhu, L. Z. 2014. Transformation, morphology, and dissolution of silicon and carbon in rice straw-derived biochars under different pyrolytic temperatures. Environ. Sci. Technol., 48(6): 3411-3419.

Xie, G. H., Wang, X. Y. and Ren, L. T. 2010. China's crop residue resources evaluation. Chin. J. Biotechnol., 26(7): 855-863.

Yang, Y. G., Liu, C. Q., Wu, P., Zhang, G. P. and Zhu, W. H. 2003. Zinc smelting is an important factor leading to heavy metal accumulation in soils and sediments in Hezhang County, Guizhou Province. Acta Mineral. Sin., (3): 255-262.

Yu, X. H., Luo, Q. L., Pan, J., Han, Y. Q. and Zhang, Q. F. 2019. Preparation and properties of flexible supercapacitor based on biochar and solid gel-electrolyte. CIESC J., 70(9): 3590-3600.

Zhang, X. Q., Hou, G. J., Zhang, Y. H. and Zhao, Y. 2017a. Structural and physico-chemical properties of biochars prepared from different rice straws. Environ. Eng., 35(9): 122-126.

Zhang, X., Song, J., Gao, H., Zhang, Q., and Liu, G. 2017b. Assessment and modeling of Cd and Pb availability in contaminated arable soils in the mining area of Guizhou. Soils, 49(2): 328-336.

Zhao, S., Cai, X. F., Wang, J., Li, X. Y., Li, D., Zhao, S. J., Yu, X. J. and Xu, D. 2021. Research progress on the effects of raw and modified biochar on soil heavy metal pollutants. Sci. Soil Water Conserv., 19(2): 135-150.

Zhong, X., Jian, X. M., Jiang, E.CH., Sun, Y. and Wang, M. F. 2019. Structure and properties of rice husk biochar/acetate starch-urea starch composite films. Acta Mater. Compos. Sin., 36(7): 1746-1752.

Zhu, Q. L., Cao, M., Zhang, X. B., Tao, K., Ke, Y. C. and Meng, L. 2021. Physicochemical and infrared spectroscopic properties of gramineae plants biochar at different pyrolysis temperatures. Biomass Chem. Eng., 55(4): 21-28.